Hindawi
International Journal of Antennas and Propagation
Volume 2019, Article ID 1371285, 10 pages
https://doi.org/10.1155/2019/1371285

Research Article

A Novel Nonlinear LPDA Design for HF Direction Finding

Xiaofei Ren,[1,2] **Hu Li**,[2] **and Shuxi Gong**[1]

[1]*National Key Laboratory of Antennas and Microwave Technology, Xidian University, Xi'an, Shaanxi 710071, China*
[2]*China Research Institute of Radiowave Propagation, Qingdao, Shandong 266107, China*

Correspondence should be addressed to Xiaofei Ren; renxf_1981@163.com

Received 5 October 2018; Accepted 15 November 2018; Published 17 February 2019

Academic Editor: Giorgio Montisci

A novel design of log-periodic dipole array (LPDA) for high-frequency direction finding (DF) is presented. The traditional Carrel method employs fixed values of scale factor and spacing factors in LPDA designs. Here, we propose a design method which uses the continuous change of both the scale factor and the spacing factor so that the length of the dipoles and the space between dipoles vary nonlinearly. One advantage of our design is that the effective distance between the phase center position and the feed point of LPDA can be increased. So the effective radius of the circularly disposed antenna array (CDAA) composed of LPDA is extended, which is important for improving the accuracy of the DF system. Both the simulation and measurement results show that the proposed LPDA achieves larger effective distance and higher gain compared to that using the traditional Carrel method. The proposed LPDA also shows characteristics of wideband impedance matching. The antenna has been successfully applied to practical HF direction finding system.

1. Introduction

A log-periodic dipole array is widely used in communication and radar due to its advantages such as wideband, high gain, and high directivity [1–3]. In order to implement high-sensitivity direction finding for HF wave signals in the range of 0–360 degrees, the DF array employs the circularly disposed antenna array (CDAA) consisting of LPDAs in the XOY plane. The beam of each antenna points to the center of the circle. One example is the product of DF system TCI model 402/410 from TCI company, USA [4]. In direction finding, it is important to make the effective radius of the array as large as possible for improving the DF accuracy [5]. For the circularly disposed antenna array (CDAA) composed of LPDAs, the effective radius of the DF array is defined as the distance between the phase center of the LPDA and the center of the circle.

One simple method is to increase the physical radius of the DF array. However, it makes the effective radius of the DF array very large at high frequency, which leads to the ambiguousness of the DF results [6]. In practice, due to the limited space for DF array installation, the size of the array is always limited to a certain range. In fact, as the frequency increases, the phase center of the LPDA moves toward the direction of the short dipole [7]. According to the dependent relationship between the phase center of LPDA and the frequency, another method is to increase the distance from the phase center to the feed point by controlling the active region position of LPDA. Thus, the effective radius of the DF array composed of LPDAs is expanded, which provides a favorable condition for direction finding.

The classical methods of the LPDA design use the Carrel method [8, 9]. The fixed scale factor (τ) and spacing factor (σ) are employed. The antenna geometric structure is varied linearly with the fixed scale parameter. The LPDA meets the requirements of a good voltage standing wave ratio, gain, and directivity by selecting the appropriate parameters. Pavlos et al. compared several evolutionary algorithms for LPDA optimization [10]. Yang et al. improved the high-frequency truncation effect by changing the scale factor [11]. Li et al. used the LPDA as a feed source to improve the working bandwidth and gain of the reflector array antenna by utilizing the characteristic that the phase center of the antenna moves with the frequency [12]. Jin et al. proposed the calculation method of the phase center of the LPDA in [13]. Chang et al. reduced the length of the dipoles of LPDA

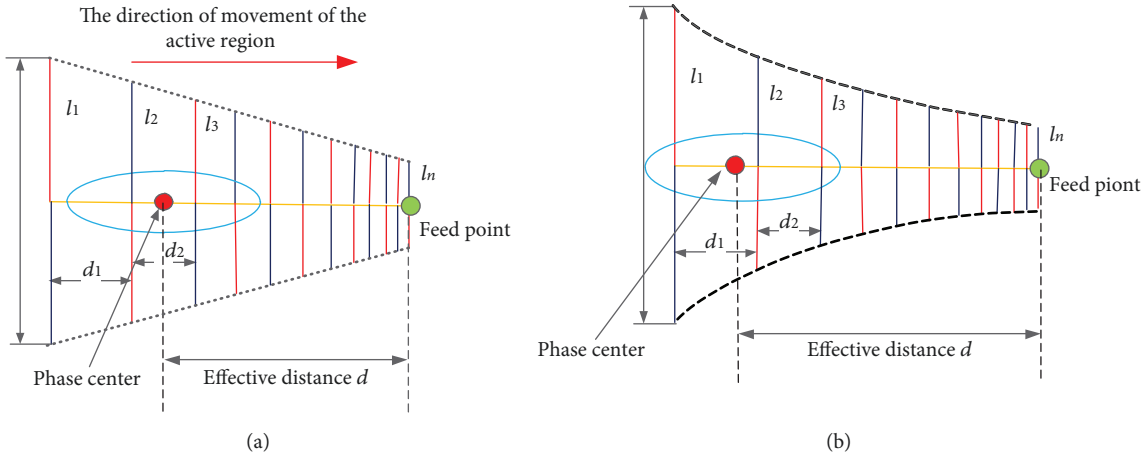

Figure 1: The schematic diagram of the effective distance d of LPDA: (a) the traditional LPDA and (b) the proposed LPDA.

by media loading [14]. And T-shaped top loadings are used to reduce the length in [15, 16]. Unlike conventional Carrel LPDA geometries, Zaharis et al. proposed an exponential log-periodic antenna design method and used the PSO (particle swarm optimization) method to optimize the parameters of the LPDA [17]. Sammeta et al. introduced a quasiplanar log-periodic antenna composite with greatly extended bandwidth of a baseline printed 4-arm log-periodic topology [18]. A new LPDA with uniform spacing and uniform height is proposed in [19]. Compared with traditional Carrel antennas, these studies have improved the antenna performance, such as VSWR, gain, and SLL.

To the best of the authors' knowledge, there is no published work that controls the phase center of the LPDA antenna. This paper presents a new design method of the LPDA antenna for high-accuracy DF application. Different from the Carrel method, we use the continuous variation of the scale factor (τ) and the spacing factor (σ). The active region of the LPDA antenna is controlled by the nonlinear variation of both the length of dipoles and the spacing between dipoles. A smaller τ factor is used at lower frequency, and a larger τ factor is used at higher frequency. Because of the smaller τ factor at a lower frequency region, the antenna size is compressed. Thus, more space is saved and the gain is improved for higher frequency. The advantage of this design is that the distance between the phase center and the feed point is increased without increasing the boom length of the LPDA, which is important to improve the accuracy of DF systems. The designed LPDA operates at 2 MHz–30 MHz, the VSWR is less than 2.0, and typical gain is 13 dBi in the array.

This paper is organized as follows. In Section 2, we discuss the new nonlinear LPDA and the DF antenna array composed of the designed antenna. The simulation and experimental verification results are presented in Section 3, and conclusions are finally given in Section 4.

2. Nonlinear LPDA Design

2.1. Nonlinear LPDA Design Method. Figure 1 shows the schematic diagram of the effective distance between the antenna phase center and the feed point in the LPDA. Both the traditional LPDA and the proposed LPDA are shown. The effective distance d of an LPDA is defined as the distance from the phase center to the feed point, as shown in Figure 1.

The length of dipoles of traditional LPDA varies according to the following formula:

$$l_n = l_1 \tau^{n-1}, \quad n = 1, 2, \ldots, N, \tag{1}$$

where τ is the scale factor which is less than 1 and l_1 is the longest dipole of the LPDA.

The length of the dipoles decreases gradually according to fixed parameters τ, and the corresponding active region moves gradually towards the direction of the shorter dipoles. The corresponding resonance frequency is as follows:

$$\ln f_n = \ln f_1 - (n-1) \ln \tau, \quad n = 1, 2, \ldots, N. \tag{2}$$

The logarithm of frequency changes linearly according to the order of dipole n with the slope of $\ln \tau$. The smaller the τ is, the faster frequency changes with n. The antenna goes through more resonant frequencies with fewer dipoles. Along the direction, the active region moves less distance. Conversely, the larger the τ is, the more dipoles the active region goes through. However, the length of the antenna becomes lager.

The objective of our research project is to increase the effective distance and achieve higher gain of the LPDA with the limitation of the antenna length.

In order to achieve this objective, the different active region needs different scale factors. When n is small, small scale parameters are used. On the other hand, when n is large, large scale parameters are adopted. In order to make the performance of the LPDA stable, we use continuously the scale factor changing method. The new method is as below:

$$l_n = l_1 \tau_0^{(n-1)^\kappa}, \quad n = 1, 2, \ldots, N, \tag{3}$$

where $0 < \kappa \leq 1$.

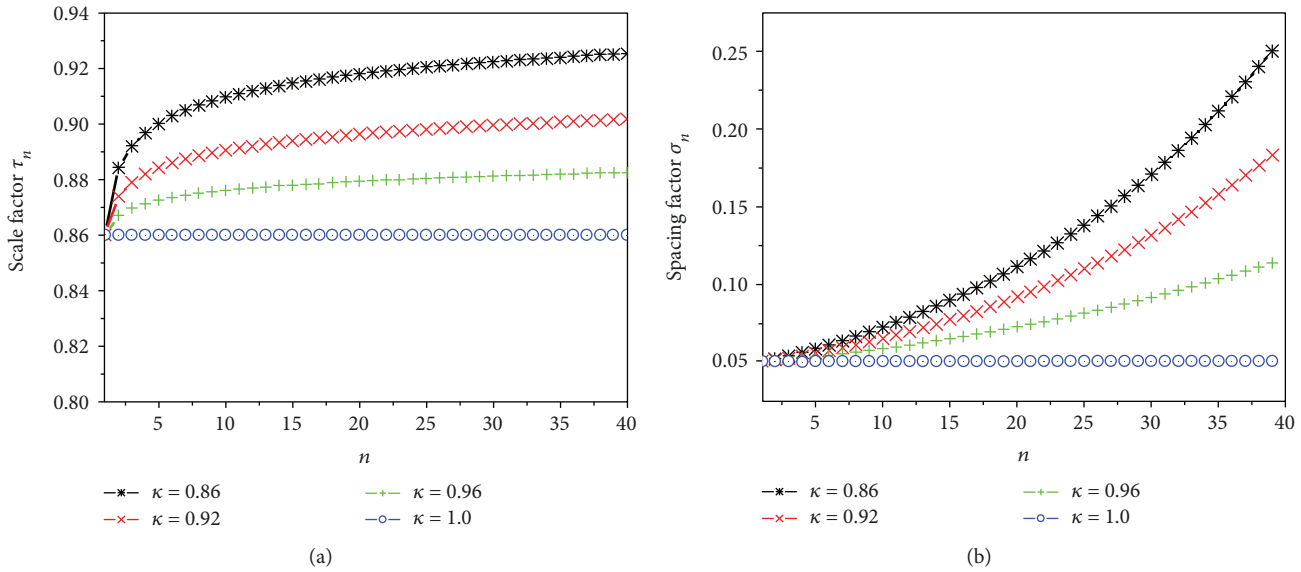

FIGURE 2: The scale factor and spacing factor of nonlinear LPDA change curve: (a) scale factor change curve ($\tau_0 = 0.86$) and (b) spacing factor change curve ($\tau_0 = 0.86$ and $\sigma_0 = 0.051$).

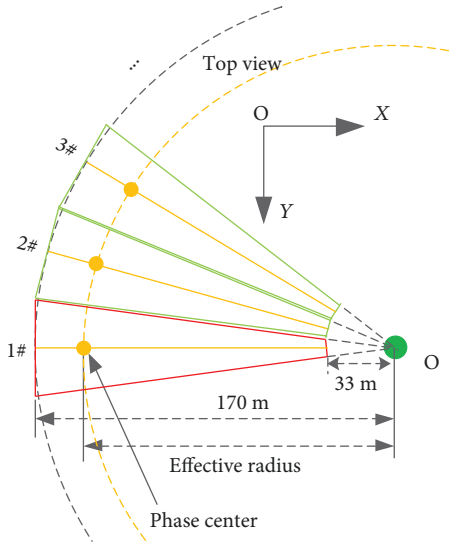

FIGURE 3: The limited area (red color-marked region) of the LPDA in the circular array.

Formula (3) can be written by applying a logarithm:

$$\ln l_n = \ln l_1 + (n-1)^{\kappa} \ln \tau_0, \quad n = 1, 2, \ldots, N. \tag{4}$$

It can be seen that the length of the dipole cannot obey the linear rule. The resonant frequency is

$$\ln f_n = \ln f_1 - (n-1)^{\kappa} \ln \tau_0, \quad n = 1, 2, \ldots, N. \tag{5}$$

Considering the change rate of resonant frequency, we make a difference operation.

$$\Delta \ln f_n = \ln f_{n+1} - \ln f_n = -[n^{\kappa} - (n-1)^{\kappa}] \ln \tau_0. \tag{6}$$

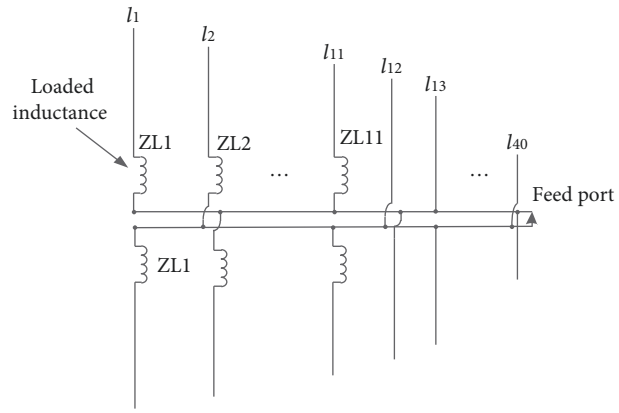

FIGURE 4: The schematic diagram of inductance lumped loading.

The change rate of resonant frequency reflects the movement rate of the active region, which is relative to the position of the dipole. There is a different change rate at a different dipole position. In a special case, when $\kappa = 1$, the change rate of resonant frequency is a constant which is $\ln \tau_0$. The active region moves along the direction of the short dipole at a fixed rate. It is a traditional LPDA.

By using the new transformation, the scale factor continuously changes on each pair of dipoles.

$$\tau_n = \frac{l_{n+1}}{l_n} = \tau_0^{\,n^{\kappa} - (n-1)^{\kappa}}, \quad n = 1, 2, \ldots, N-1. \tag{7}$$

When n is small, τ_n is small, and when n is large, τ_n is large. The change of the scale factor is controlled by the κ factor. When $\kappa = 1$, $\tau_n = \tau_0$.

We can control the active region and make it move at different moving rates at a different position on the assembly line. Thus, the effective distance d of the LPDA can be

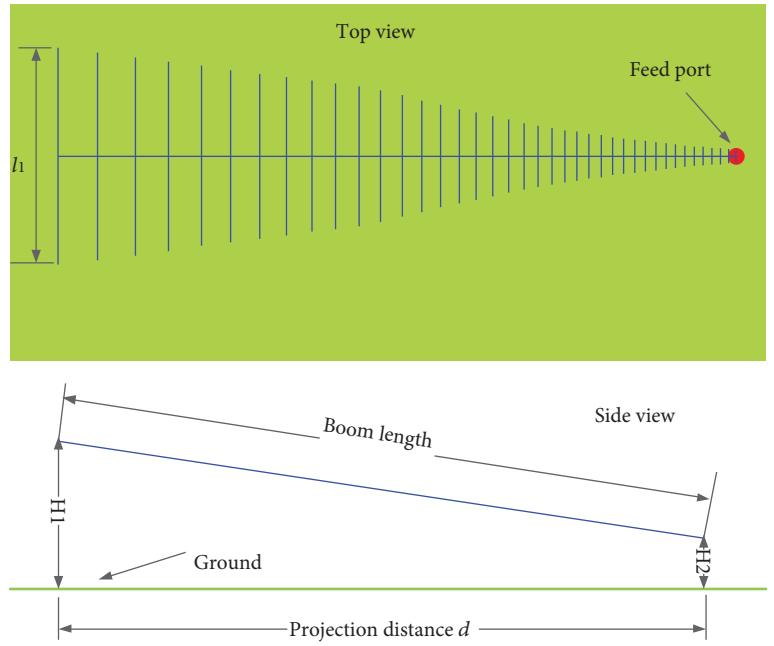

Figure 5: The model of the proposed nonlinear LPDA shortening dipoles 1 to 11.

Table 1: The parameters of the proposed nonlinear LPDA.

Parameter	Value	Parameter	Value
N	40	l_1	44.9 m
τ_0	0.866	l_{40}	2.9 m
σ_0	0.051	D	136.9 m
κ	0.86	H1	43 m
Boom length	139.8 m	H2	12 m

Table 2: The parameters of inductance loading in the LPDA.

Parameter	Value	Parameter	Value
ZL1	28.5 μH	ZL7	7.0 μH
ZL2	25.2 μH	ZL8	5.0 μH
ZL3	23.0 μH	ZL9	3.4 μH
ZL4	19.0 μH	ZL10	2.1 μH
ZL5	14.0 μH	ZL11	0.8 μH
ZL6	11.0 μH		

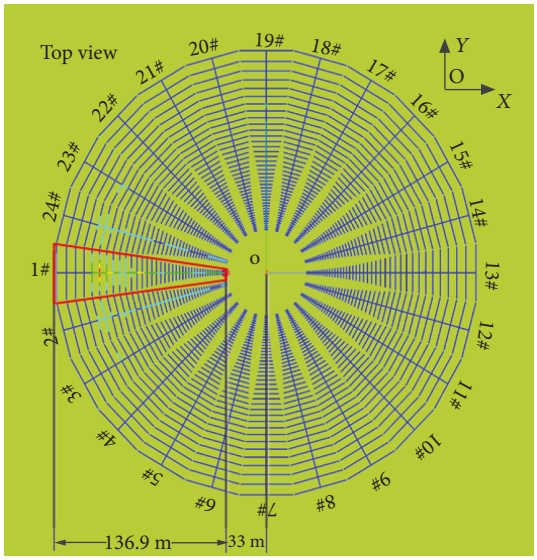

Figure 6: The circular array composed of a nonlinear LPDA. The red border is the design range of the element.

controlled. The length of the dipole in the LPDA varies nonlinearly, as shown in Figure 1(b).

To make the spacing factor also continuously change, we construct a new relationship between the dipole spacing of the LPDA.

$$d_n = d_1 \tau_n^{(n-1)^\kappa} = 2\sigma_0 l_1 \tau_n^{(n-1)^\kappa}, \quad n = 1, 2, \ldots, N-1. \tag{8}$$

So the new spacing factor is

$$\sigma_n = \frac{d_n}{2l_n} = \sigma_0 \left(\frac{\tau_n}{\tau_0}\right)^{(n-1)^\kappa}, \quad n = 1, 2, \ldots, N-1. \tag{9}$$

When $n = 1$, $\sigma_1 = \sigma_0 = d_1/2l_1$, which are considered to be the initial parameters that have to be defined. The benefit of this transformation is that the spacing factor is automatically nonlinear. If the scale factor τ_n becomes larger, then the spacing factor σ_n becomes larger as well. The impedance and gain of the LPDA are more stable.

If the initial parameters τ_0 and σ_0 and κ factor are given, the LPDA can be designed. Obviously, the new design method has one more degree of freedom than the traditional Carrel design method. This benefits the LPDA design.

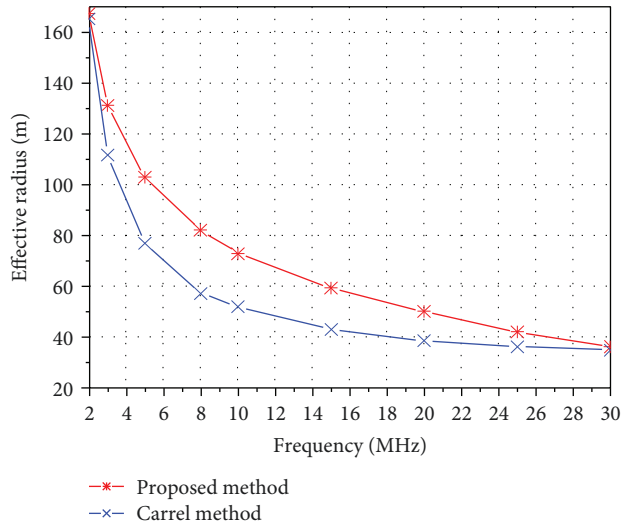

Figure 7: The effective radius variation curve with frequency.

Figure 2 shows the variation curve of the scale factor and spacing factor with dipole n under different κ factors.

2.2. The Nonlinear LPDA Design for HF Direction-Finding. Using the method presented above, we designed a circularly disposed antenna array (CDAA) composed of nonlinear LPDAs that operates at 2–30 MHz for HF direction finding. It is required that the horizontal projection distance between the longest dipole in the LPDA and the center of the circle is 170 m (the LPDA tilts with the ground). The distance between the feed point and the center of the circle is 33 m. The angle of the adjacent antenna is 15°. The circular array is composed of 24 elements of a nonlinear LPDA. The element is limited to the red area as shown in Figure 3. One of the benefits of circular arrays is that the mutual coupling of the elements in the array is exactly the same. In the CDAA, the effective radius of the DF array is defined as the horizontal distance between the phase center of the LPDA and the center of the circle.

In order to increase the effective radius, it is not recommended to choose κ to be 1; however, if κ is too small, the gain in low frequency of the antenna decreases significantly. According to the operating frequency of the antenna, the length of the longest dipole is a half wavelength which corresponds to the lowest working frequency. The initial parameters that have been chosen are $\tau_0 = 0.866$, $\sigma_0 = 0.051$, and $\kappa = 0.86$, respectively. Dipoles are filled in the design area as many as possible to form a reasonable effective radius and ensure the performance of the antenna in the whole frequency range. The total number of the dipoles N is 40.

Due to the required baseline of the array, some longer dipoles need to be cut short. This result in the resonant frequency is changed. To avoid this effect, an inductance-lumped loading method is used to maintain the resonant frequency, as shown in Figure 4. According to the array structure, 11 pairs of dipole need to be shortened and lumped inductors are applied to these dipoles. Because the HF antenna is affected by the ground, the LPDA needs to have an angle of inclination to ensure that the electric height of the antenna above the ground does not change drastically in a wide frequency band. The model of the designed nonlinear LPDA is shown in Figure 5. The parameters of the proposed nonlinear LPDA are shown in Table 1, and the inductance loading parameters are shown in Table 2.

Through this design, the entire antenna size is exactly filled in the required area, forming a reasonable and compact structure. The model of the circularly disposed array composed of a nonlinear LPDA is shown in Figure 6.

3. Simulated and Measured Results

3.1. Comparison with the Traditional Carrel LPDA. In order to verify the proposed nonlinear LPDA design method, we compared it with the traditional Carrel LPDA. The physical length of the antenna designed by the Carrel method is also 139.8 m, and the horizontal projection distance is 136.9 m. The scale factor and spacing factor are fixed to be $\tau = 0.92$ and $\sigma = 0.0776$, respectively. The total number of dipoles is also 40. The horizontal projection distance between the two antennas' shortest dipole and the coordinate origin is 33 m, pointing to the X direction. The simulation is performed using FEKO. Figure 7 shows the variation of the effective radius (the horizontal distance between the phase center of the LPDA and the coordinate origin) with frequency. We can see that the effective radius of the nonlinear LPDA is obviously larger than Carrel's and the effective radius is decreasing as the frequency is increasing. This characteristic maintains a reasonable electrical effective radius in DF array. The results shown in Figure 7 demonstrate the effectiveness of the proposed method in controlling the effective radius (effective distance). The comparison with the Carrel antenna and proposed antenna (nonlinear LPDA) is shown in Table 3.

Figure 8 shows the current distribution of the Carrel antenna and the proposed LPDA. It can be seen from the current distributions that the active region of the proposed LPDA is further away from the feed port than that of the traditional Carrel LPDA. In Figure 8, in order to compare the current distribution of the two antennas, only the antennas are aligned and displayed. In fact, the current distributions of the two types of antennas were calculated independently.

Compared with the Carrel antenna, it can be seen that the gain of the proposed nonlinear LPDA is about 1 dB greater than the Carrel antenna above 4 MHz. At lower frequency, because of the smaller scale factor and inductance load used, the antenna size is compressed, so the gain is smaller than the Carrel antenna. However, more space is saved in the high-frequency zone and the larger τ factor is used. Therefore, the gain in high frequency can be improved. Because τ factor is continuous changed from small to large, the active region is further away from the feed point. So the effective radius is larger than the Carrel antenna, which employs a fixed τ factor in all

Table 3: Comparison with the Carrel antenna and proposed antenna.

Frequency	Effective radius		Beamwidth		Gain	
	Carrel method	Proposed nonlinear method	Carrel method	Proposed nonlinear method	Carrel method	Proposed nonlinear method
2 MHz	165.4 m	167.4 m	80°	86°	10.3 dBi	9.2 dBi
4 MHz	91.6 m	118.3 m	74°	76°	11.3 dBi	11.1 dBi
8 MHz	57.3 m	82.1 m	70°	64°	12.1 dBi	12.8 dBi
12 MHz	49.2 m	68.7 m	66°	62°	12.6 dBi	13.6 dBi
20 MHz	38.6 m	50.2 m	70°	60°	12.8 dBi	13.7 dBi
25 MHz	36.3 m	42.0 m	68°	60°	12.9 dBi	13.5 dBi
30 MHz	34.9 m	36.2 m	68°	64°	12.7 dBi	13.2 dBi

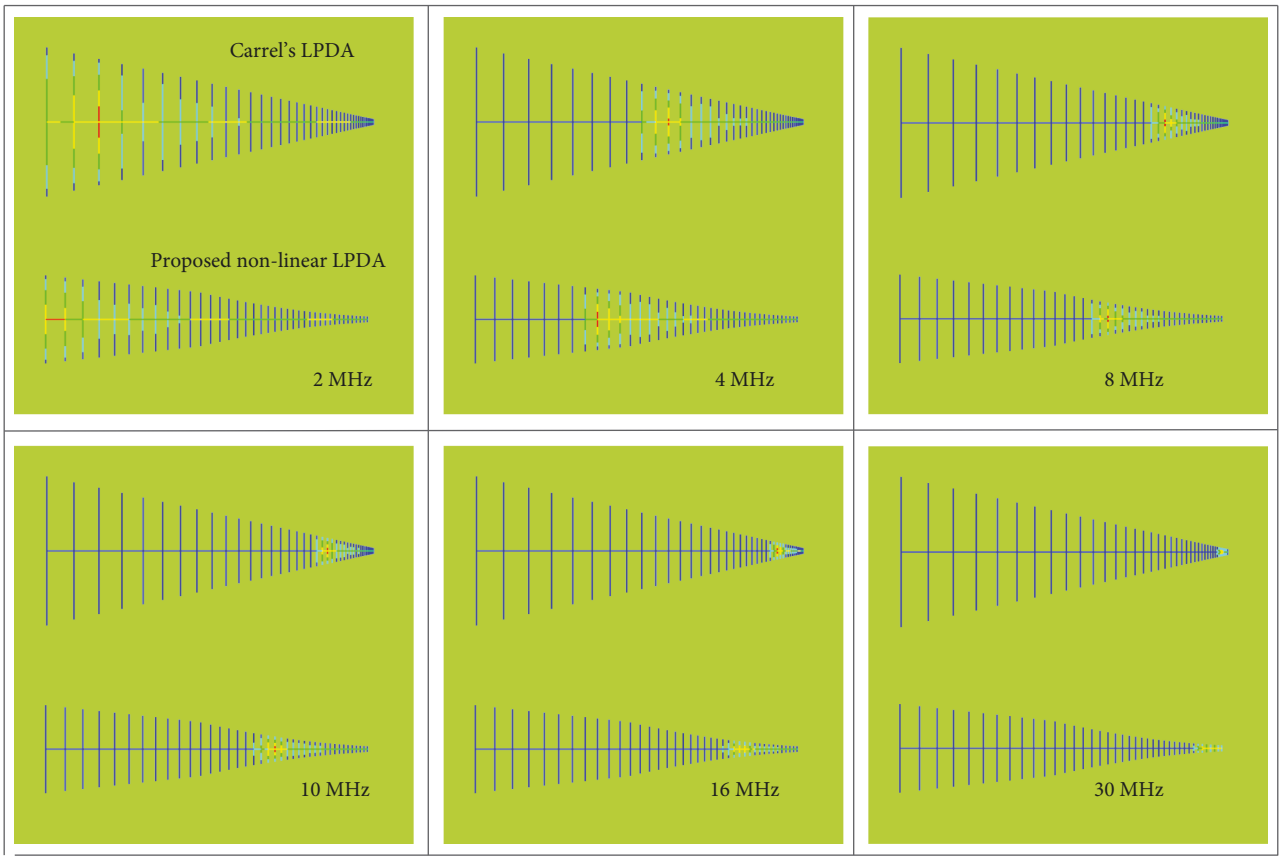

Figure 8: Comparison of the current distribution between the Carrel antenna and proposed LPDA.

operating frequency bands. The performance of the proposed nonlinear LPDA is improved.

3.2. Measurement of the HF LPDA. The circular direction-finding array using the proposed nonlinear LPDA was fabricated and implemented in practical applications, as shown in Figure 9. The circular array consists of 24 LPDAs with an angle of 15 degrees between adjacent elements, forming a compact circular array. The measured results reflect the characteristics of the element in the array, concluding the mutual coupling.

For HF antennas, unmanned aerial vehicles at a low altitude of 300 m were used for testing. The test distance is 3 km,

Figure 9: The fabricated direction finding array by using the proposed nonlinear LPDA.

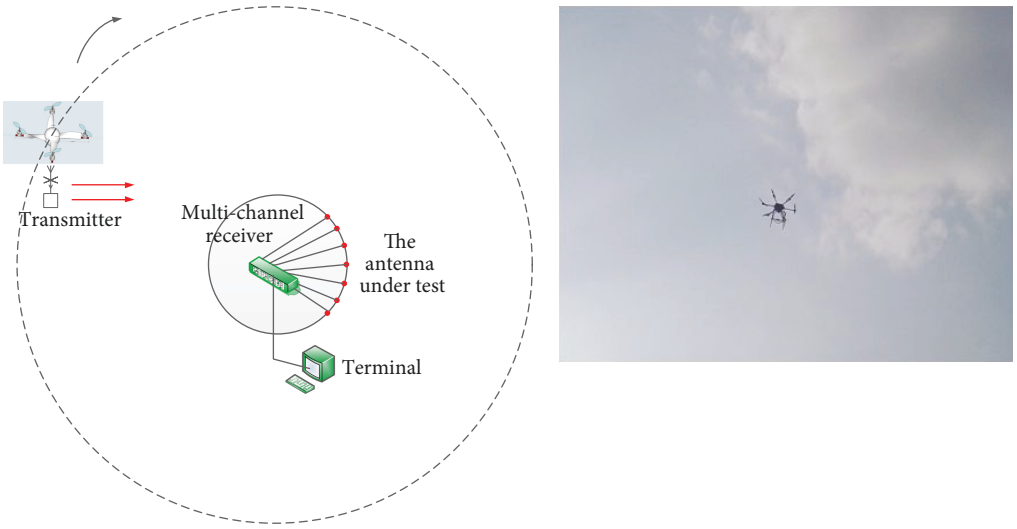

Figure 10: (a) Antenna measurement diagram and (b) the unmanned aerial vehicles at an altitude of 300 m.

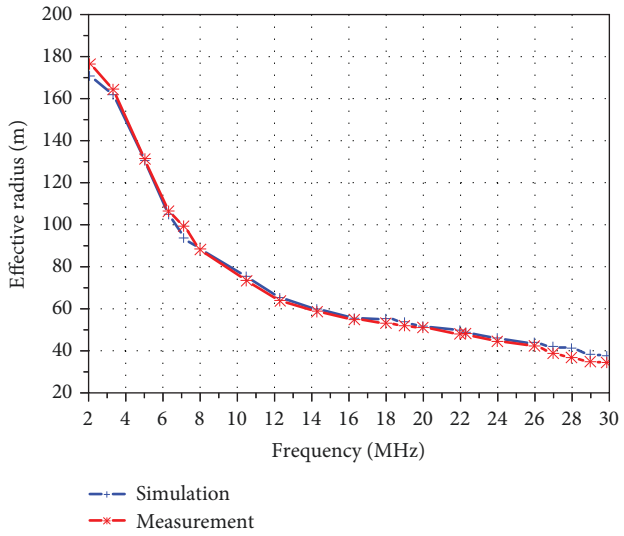

Figure 11: The variation curve of the effective radius with frequency in the measurement.

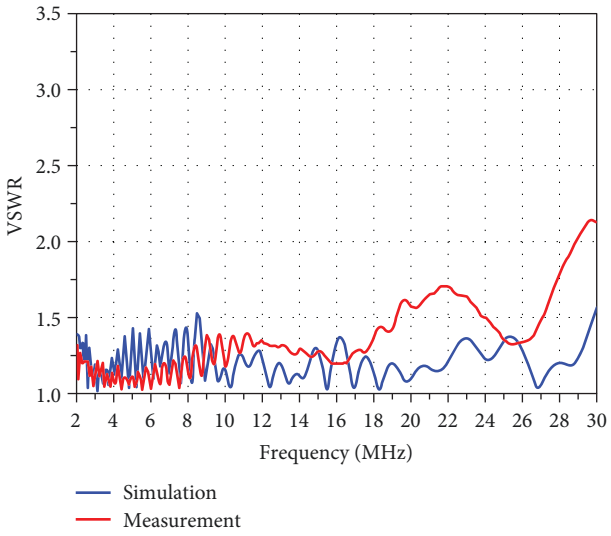

Figure 12: The variation curve of VSWR with frequency.

which was approximate in the far field of the element antenna. A remotely controlled transmitter and a horizontal loop antenna are mounted on the unmanned aerial vehicles. And a small GPS antenna mounted on top provides location information. The total weight of the transmitting system is 5 kg. The UAV provides a moving source. The antennas to be measured are connected to the multichannel receiver. The amplitude and phase information of the receiving signal were extracted from the multichannel receiver and can be saved in the industrial personal computer (IPC). We can receive the relative amplitude data and phase data with the UAV flying at a certain altitude. Thus, we can obtain the amplitude pattern and the phase difference among the LPDAs. The diagram of the test system is shown in Figure 10.

The actual effective radius of the array (including mutual coupling) can be obtained using a least square method by measuring the phase difference among the receiving antennas. According to the characteristic of the CDAA, the theoretical relation of phase difference between the mth and nth elements is depicted in [20].

$$\Delta\psi_{m,n} = kr_0 \sin\theta[\cos(\phi - \beta_m) - \cos(\phi - \beta_n)], \quad (10)$$

where r_0 is the effective radius, $k = 2\pi/\lambda$, λ is the wavelength of the test signal, (θ, ϕ) is the position of transmitter, and β_m and β_n are the angles between the mth and nth elements and the X axis (Figure 6.). To obtain the actual effective radius, the least square method is adopted according to the measured phase difference.

$$\varepsilon = \sum_{i=1}^{N-1} \left|\Delta\tilde{\psi}_{i,N} - \Delta\psi_{i,N}\right|^2, \quad (11)$$

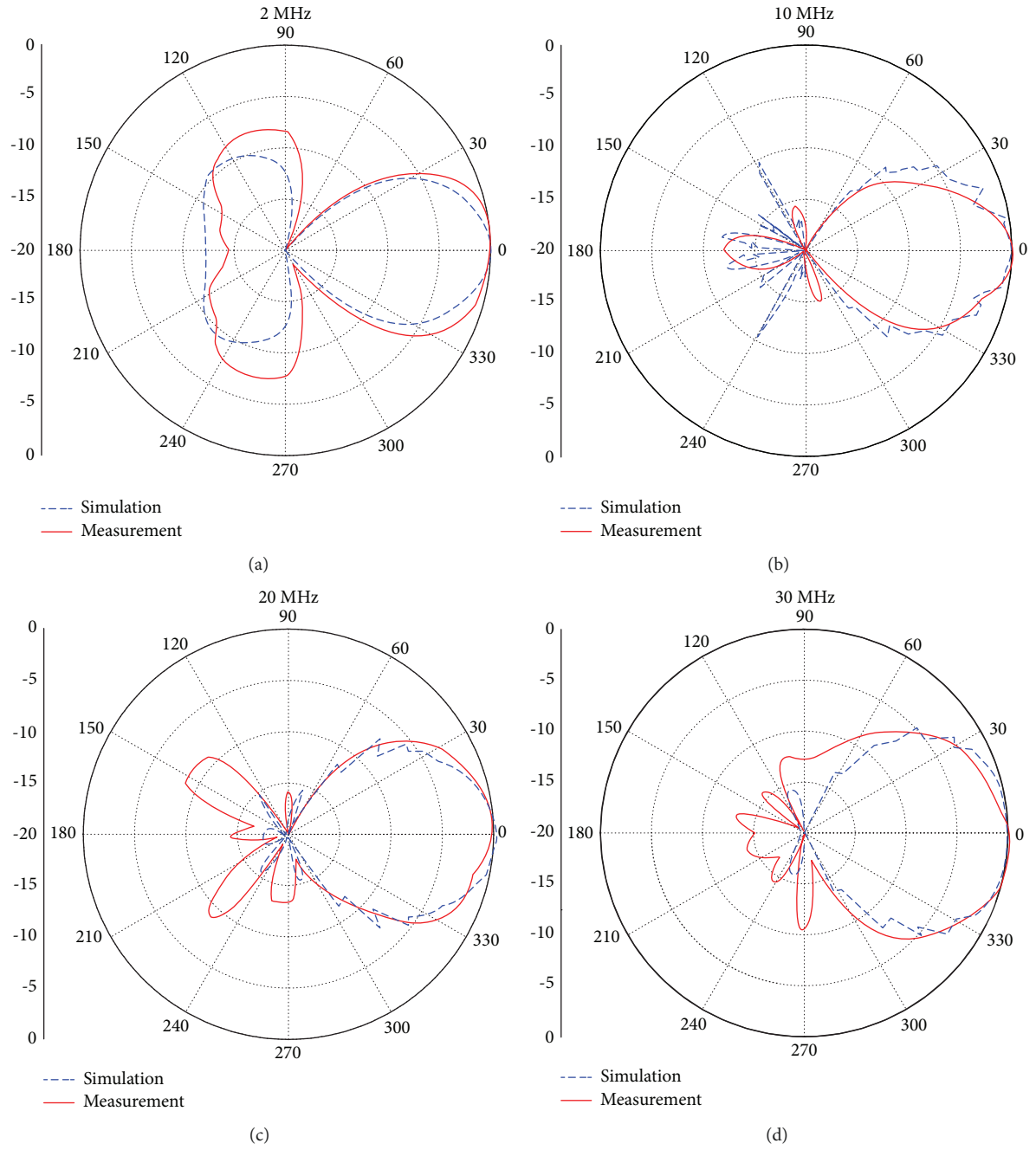

Figure 13: The measured horizontal pattern with the elevation angle of 8 degrees.

where $\Delta\tilde{\psi}_{i,N}$ is the phase difference measured between the ith and nth elements and $\Delta\psi_{i,N}$ is the theoretical phase difference according to (10), which contains the effective radius. By finding the minimum ε, the effective radius is obtained.

Due to the limitation of flight height, we characterized the antenna with the elevation angle of 8 degrees. To make a fair comparison, we compare the measured result with the theoretical simulation results of the same elevation angle. Figure 11 shows the measured results of the effective radius in the CDAA.

It can be seen that the measured effective radius is in good agreement with the theoretical simulation. The VSWR curve of the nonlinear LPDA is shown in Figure 12. Figure 13 shows the measured radiation patterns in the horizontal plane with the elevation angle of 8 degrees.

For the DF antenna array, the phase difference of the baseline between the LPDAs should be considered. It is related to the effective radius of the CDAA [21]. Figure 14 shows the phase difference of different baselines in the CDAA composed of the proposed nonlinear LPDAs.

The results indicate that the phase difference of the measurement is consistent with the simulation. When the incoming wave is from 0°, the phase difference of the 2# baseline and 3# baseline is 0 degree. Since the angle between adjacent

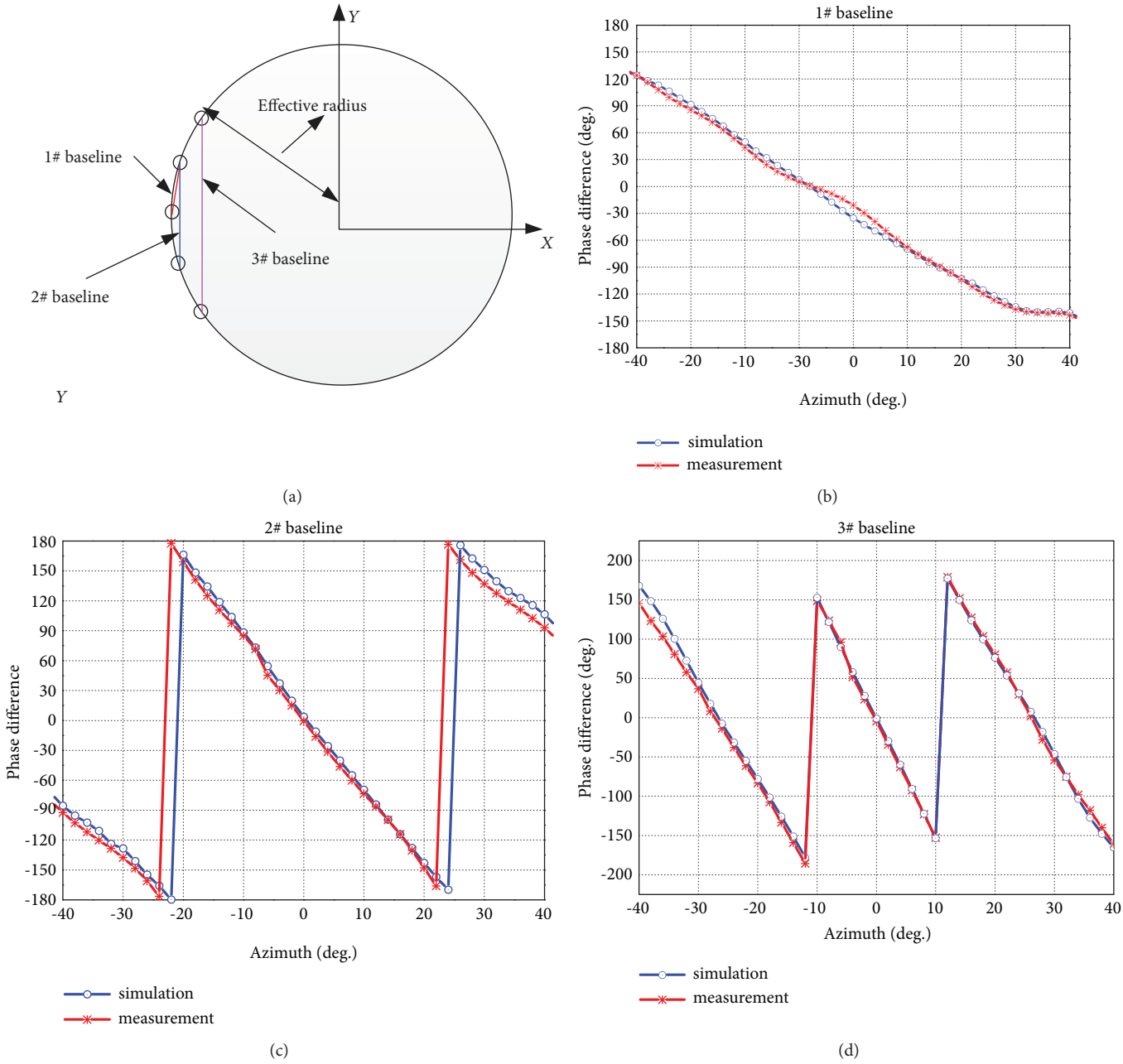

FIGURE 14: The phase difference of the different baselines at 10 MHz: (a) the definition of the baseline in the circular array and (b–d) phase difference of baselines 1~3, respectively.

antennas is 15 degrees, the phase difference of the 1# baseline is 0 degree when the incoming wave is from −7.5° (the normal of the baseline 1# point to −7.5°). The results of simulation and measurement accord with the physical law.

4. Conclusions

A new nonlinear LPDA design method is presented in the paper. The length and spacing of the dipole are changed according to the nonlinear rule to control the position of the phase center of the LPDA. The scale factor and spacing factor of the LPDA are continuously changed to increase the effective distance and guarantee the performance of the antenna. The simulation and measurement results show that the proposed nonlinear LPDA has good performance for high sensitive HF direction-finding applications. The CDAA composed of the nonlinear LPDA has been successfully used in a practical HF direction-finding system.

Data Availability

The data used to support the findings of this study are available from the corresponding author upon request.

Conflicts of Interest

The authors declare that they have no conflicts of interest.

Acknowledgments

This research is supported by the China Research Institute of Radiowave Propagation. The authors would like to thank Prof. Li and Dr. Cui for the useful discussions and measurement.

References

[1] A. Chauloux, F. Colombel, M. Himdi, J.-L. Lasserre, and P. Pouliguen, "Low-return-loss printed log-periodic dipole antenna," *IEEE Antennas and Wireless Propagation Letters*, vol. 13, pp. 503–506, 2014.

[2] X. Gao, Z. Shen, and C. Hua, "Conformal VHF log-periodic balloon antenna," *IEEE Transactions on Antennas and Propagation*, vol. 63, no. 6, pp. 2756–2761, 2015.

[3] G. A. Casula, G. Montisci, P. Maxia, G. Valente, A. Fanti, and G. Mazzarella, "A low-cost dual-band CPW-fed printed LPDA for wireless communications," *IEEE Antennas and Wireless Propagation Letters*, vol. 15, pp. 1333–1336, 2016.

[4] I TCI International, "TCI model 402/410," https://www.tcibr.com/product/tci-model-402410/.

[5] B. R. Jackson, S. Rajan, B. J. Liao, and S. Wang, "Direction of arrival estimation using directive antennas in uniform circular arrays," *IEEE Transactions on Antennas and Propagation*, vol. 63, no. 2, pp. 736–747, 2015.

[6] E. Kornaros, S. Kabiri, and F. De Flaviis, "A novel model for direction finding and phase center with practical considerations," *IEEE Transactions on Antennas and Propagation*, vol. 65, no. 10, pp. 5475–5491, 2017.

[7] C. Barès, C. Brousseau, L. le Coq, and A. Bourdillon, "Effect of antenna phase centre displacement on FM-CW measurements: application to radar system," *Electronics Letters*, vol. 39, no. 11, pp. 867-868, 2003.

[8] R. Carrel, "The design of log-periodic dipole antennas," in *IRE International Convention Record*, pp. 61–75, New York, NY, USA, 1961.

[9] G. de Vito and G. Stracca, "Comments on the design of log-periodic dipole antennas," *IEEE Transactions on Antennas and Propagation*, vol. 21, no. 3, pp. 303–308, 1973.

[10] P. I. Lazaridis, E. N. Tziris, Z. D. Zaharis et al., "Comparison of evolutionary algorithms for LPDA antenna optimization," *Radio Science*, vol. 51, no. 8, pp. 1377–1384, 2016.

[11] J. Yang, S. C. Wu, and H. T. Gao, "Study of log periodic dipole antennas," *Journal of Wuhan University*, vol. 49, no. 1, pp. 141–144, 2003.

[12] W. Li, S. Gao, L. Zhang, Q. Luo, and Y. Cai, "An ultra-wide-band tightly coupled dipole reflectarray antenna," *IEEE Transactions on Antennas and Propagation*, vol. 66, no. 2, pp. 533–540, 2018.

[13] Y. Jin, X. Ren, H. Ji, and S. He, "Variable phase center of log-periodic dipole antenna in full space," *Chinese Journal of Radio Science*, vol. 22, pp. 229–233, 2007.

[14] L. Chang, S. He, J. Q. Zhang, and D. Li, "A compact dielectric-loaded log-periodic dipole array (LPDA) antenna," *IEEE Antennas and Wireless Propagation Letters*, vol. 16, pp. 2759–2762, 2017.

[15] J. Chen, J. Ludwig, and S. Lim, "Design of a compact log-periodic dipole array using T-shaped top loadings," *IEEE Antennas and Wireless Propagation Letters*, vol. 16, pp. 1585–1588, 2017.

[16] A. Kyei, D.-U. Sim, and Y.-B. Jung, "Compact log-periodic dipole array antenna with bandwidth-enhancement techniques for the low frequency band," *IET Microwaves, Antennas & Propagation*, vol. 11, no. 5, pp. 711–717, 2017.

[17] Z. D. Zaharis, I. P. Gravas, T. V. Yioultsis et al., "Exponential log-periodic antenna design using improved particle swarm optimization with velocity mutation," *IEEE Transactions on Magnetics*, vol. 53, no. 6, pp. 1–4, 2017.

[18] R. Sammeta and D. S. Filipovic, "Quasi frequency-independent increased bandwidth planar log-periodic antenna," *IEEE Transactions on Antennas and Propagation*, vol. 62, no. 4, pp. 1937–1944, 2014.

[19] Q. Song, Z. Shen, and J. Lu, "Log-periodic monopole array with uniform spacing and uniform height," *IEEE Transactions on Antennas and Propagation*, vol. 66, no. 9, pp. 4687–4694, 2018.

[20] X. Ren and S. X. Gong, "Direction of arrival estimation based on heterogeneous array," *Progress In Electromagnetics Research M*, vol. 69, pp. 97–106, 2018.

[21] J.-H. Lee and J.-M. Woo, "Interferometer direction-finding system with improved DF accuracy using two different array configurations," *IEEE Antennas and Wireless Propagation Letters*, vol. 14, pp. 719–722, 2015.